

Amperometric ion-selective electrode. Voltammetric theory and analytical applications at high concentration and trace levels^{☆,☆☆}

Mitsugi Senda *, Hajime Katano, Masayuki Yamada

Department of Bioscience, Fukui Prefectural University, Matsuoka-cho, Fukui 910-1195, Japan

Received 19 October 1998; received in revised form 9 February 1999; accepted 16 February 1999

Abstract

The theory of normal pulse voltammetry (NPV) and cyclic potential sweep voltammetry (CV) of the amperometric ion-selective electrodes (AISEs) based on the ionophore-assisted transfer of ions across polarized organic solvent or oil|water (O|W) interfaces is discussed. The numerical solution of the resulting integral equations has been used to show how their voltammograms vary with the ratio of the concentration of analyte ion in the W phase, that is, the test solution, to that of ionophore in the O phase, that is, the ion-sensitive membrane. Generally, the current response of the AISEs at constant ionophore concentration is not linear with respect to the concentration of analyte ion when the ratio exceeds 0.01. In order to obtain a linear calibration curve in a wide range of analyte concentrations, up to a few molar of Na⁺ ion, e.g. a new technique, called F-pulse amperometry, is proposed and experimentally verified, where a pulse voltage corresponding to the 'foot-of-wave' potential is applied and the current is sampled according to the NPV technique. When the concentration of analyte ion is very low, the stripping voltammetry technique is promising. Poly(oxyethylene)alkyl ether surfactants at ppb levels can be determined using the stripping voltammetry technique based on the electrochemical pre-concentration of the surfactants by ion-assisted transfer at the O-gel|W interface. © 1999 Elsevier Science S.A. All rights reserved.

Keywords: Ion-transfer voltammetry; Theory; Ion-selective electrode; Amperometry; High concentration analysis; Trace analysis

1. Introduction

Recent electrochemical studies on ion-transfer reactions across the interface between two immiscible electrolyte solutions, or, in short, the oil|water (O|W) interface, have shown that this interface can be polarized and that the transfer of ions taking place across the O|W interface within the polarizable potential range, or through what is called the potential window, can be studied using voltammetric or polarographic techniques. Thus, the polarizable O|W interface can function as an electrode interface which responds voltammetrically to a specified ion (or ions) that is (or are) transferable across the interface through the potential window. In other words, we have obtained an

ion-selective electrode (ISE) based on a polarizable O|W interface. According to the theory of voltammetry and polarography, there are two available types of ISEs; an amperometric ion-selective electrode (AISE) and a potentiometric ion-selective electrode (PISE). The former gives a current response which is proportional to the concentration of the analyte ion, whereas the latter gives a potential response which changes linearly with the logarithm of the activity (or concentration) of the analyte ion, see Refs. [1–3] for review. The PISEs, both in theory and applications, have been studied quite comprehensively for many decades and their practical applications have also been well recognized. On the other hand, the AISEs have recently been studied and their analytical applicability has been discussed also recently [1–10].

In order to make the O|W interface selectively responsive to a specified ion M in the W phase, that is, the test solution, in most cases a hydrophobic ionophore L which associates selectively with the specified ion M to form a hydrophobic complex LM (and,

[☆] PII of original article S0022-0728(99)00086-8.

^{☆☆} Lecture presented at the International Symposium on New Trends in Electroanalytical Chemistry, Seoul, South Korea, 10–12 September, 1998.

* Corresponding author. Fax: +81-776-616015.

E-mail address: senda@fpu.ac.jp (M. Senda)

in some cases, L_nM ($n = 2, \dots$) etc.) is added in the O phase, that is, the ion-sensing membrane. Then, the transfer of the specified ion M across the O|W interface is selectively facilitated by the formation of the complex LM in the O phase. The purpose of the present paper is to address the theory and analytical applications of normal pulse voltammetry (NPV) and cyclic potential sweep voltammetry (CV) of the ionophore(L)-assisted transfer of M ion across the O|W interface. In analytical applications, two extreme cases with reference to the range of the concentration of analyte ion are discussed. In the first case when the concentration of the analyte ion is relatively high, where the concentration of the analyte ion frequently exceeds the concentration of the ionophore, a new technique, named F-pulse amperometry, is proposed to obtain a linear calibration curve for a range of concentrations up to a few molar. Experimental results obtained with AISEs for Na^+ ion are described. In the second case when the concentration of the analyte ion is at trace level, application of the stripping voltammetry technique seems promising; the ion-transfer stripping voltammetry applied to the determination of surfactants as well as heavy metal ions, at as low as ppb level, using a thin O-gel membrane-based AISE is described.

2. Theory

Let the formation of the hydrophobic complex LM in the O phase be expressed by



with the formal formation constant, K^{O} , defined by

$$K^{\text{O}} = c_{\text{LM}}^{\text{O}} / c_{\text{M}}^{\text{O}} c_{\text{L}}^{\text{O}} \quad (2)$$

where c_i^{α} is the concentration of i ($i = \text{M}, \text{L}, \text{LM}$) species in the α ($\alpha = \text{O}, \text{W}$) phase. We also have the Nernst–Donnan equation for the transfer or partition of M ion at the O|W interface, as expressed by:

$$\Delta\phi = \Delta\phi_{\text{M}}^{\text{O}'} + (RT/zF) \ln[(c_{\text{M}}^{\text{O}})^{\circ} / (c_{\text{M}}^{\text{W}})^{\circ}] \quad (3)$$

where $\Delta\phi$ is the potential difference across the interface, $\Delta\phi_{\text{M}}^{\text{O}'}$ the formal potential of M ion transfer across the O|W interface, z the charge number, including the sign, of M ion, $(c_i^{\alpha})^{\circ}$ the surface concentration of i ($i = \text{M}, \text{L}, \text{LM}$) species in the α ($\alpha = \text{O}, \text{W}$) phase, and R , T and F are used with the usual meanings. We assume (a) that L and LM are extremely hydrophobic and their presence in the W phase can be neglected, (b) that M is extremely hydrophilic and its presence in the O phase can be neglected (that is, $K^{\text{O}} c_{\text{L}}^{\text{O}} \gg 1$ in Eq. (2)), (c) that the association and dissociation of LM complex in the O phase are very fast processes so that Eq. (2) is valid everywhere in the O phase, and (d) that the ion

transfer reaction at the O|W interface is a very fast process so that Eq. (3) is always valid at the interface. Then, the whole ion-transfer process may be expressed by



with the interfacial condition as given by

$$\Delta\phi = \Delta\phi_{\text{M}}^{\text{O}'} + (RT/zF) \ln[1/K^{\text{O}}] \\ + (RT/zF) \ln[(c_{\text{LM}}^{\text{O}})^{\circ} / (c_{\text{L}}^{\text{O}})^{\circ} (c_{\text{M}}^{\text{W}})^{\circ}] \quad (5)$$

The semi-infinite diffusion problem of M in the W phase ($x > 0$, x being the distance) and L and LM in the O phase ($x < 0$) at a stationary plane interface ($x = 0$) was solved, using the standard method [11,12], under the boundary conditions as given by Eq. (5) and other equations used usually in the semi-infinite diffusion problem, and the initial conditions that M ion is present at the concentration of $(c_{\text{M}}^{\text{W}})^*$ in the W phase while L is present at $(c_{\text{L}}^{\text{O}})^*$ in the O phase and that the applied potential E is kept at the initial potential E_i where no ion-transfer current will take place. The applied potential is related to the interfacial potential difference by [13]:

$$E = \Delta\phi + \Delta E_{\text{ref}} \quad (6)$$

where ΔE_{ref} is determined by the combination of the two reference electrodes used in the experiment (see Section 3). It can be shown that the numerical solutions for the voltammograms of NPV and CV are dependent on the parameter a defined by

$$a = (D^{\text{W}}/D^{\text{O}})^{1/2} (c_{\text{M}}^{\text{W}})^* / (c_{\text{L}}^{\text{O}})^* \quad (7)$$

where D^{W} is the diffusion coefficient of M ion in the W phase and D^{O} the common diffusion coefficient of L and LM species in the O phase.

When a is negligibly small, that is, $a \ll 1$, the voltammogram (the sampled current, I , versus applied potential, E , curve) of NPV is obtained by an analytical equation [13], the well-known equation of a reversible polarographic wave, which is expressed by:

$$I_{(\text{M})} = I_{\text{d}(\text{M})} / (1 + \exp[(zF/RT)(E_{1/2(\text{M})} - E)]) \quad (8)$$

where the limiting (diffusion) current, $I_{\text{d}(\text{M})}$, and the (reversible) half-wave potential, $E_{1/2(\text{M})}$, are given by:

$$I_{\text{d}(\text{M})} = zFA(D^{\text{W}}/\pi t_s)^{1/2} (c_{\text{M}}^{\text{W}})^* \quad (9)$$

$$E_{1/2(\text{M})} = E_{\text{M}}^{\text{O}'} + (RT/zF) \ln[(D^{\text{W}}/D^{\text{O}})^{1/2}] \\ + (RT/zF) \ln[1/K^{\text{O}}(c_{\text{L}}^{\text{O}})^*] \quad (10)$$

In these equations, $E_{\text{M}}^{\text{O}'} = \Delta\phi_{\text{M}}^{\text{O}'} + \Delta E_{\text{ref}}$ and $E = E_i + \Delta E$, ΔE being the amplitude of the pulse voltage. A is the area of the interface, that is, the electrode surface area and t_s is the sampling time. Likewise, the voltammogram (the current, I , vs. applied potential, E , or time, t , curve) of CV is obtained as a numerical solu-

tion and the peak current height, $I_{p,a(M)}$, the peak potential, $E_{p,a(M)}$, and the half-peak potential, $E_{p/2,a(M)}$, in the first positive potential sweep are expressed, respectively, by [14]:

$$I_{p,a(M)} = 0.447zFA(D^W v z F / RT)^{1/2} (c_M^W)^* \quad (11)$$

$$E_{p,a(M)} = {}_r E_{1/2(M)} + 1.11(RT/zF) \quad (12a)$$

$$E_{p/2,a(M)} = {}_r E_{1/2(M)} - 1.09(RT/zF) \quad (12b)$$

Here, the applied potential, E , is defined by $E = vt + E_i$, v being the rate of the potential sweep.

When $a > 0.01$, the voltammograms of NPV and CV are obtained as numerical solutions which are shown in Figs. 1 and 2 for several a -values. The voltammograms of CV have been obtained numerically by Beattie et al. [15]. The present numerical solutions, which were obtained by a standard method using Mathematica Version 3, are naturally the same as those by these authors [15]. These results can be summarized in good approximation as follows;

Case I: when $0 < a \leq 1$, the voltammogram of NPV is expressed by

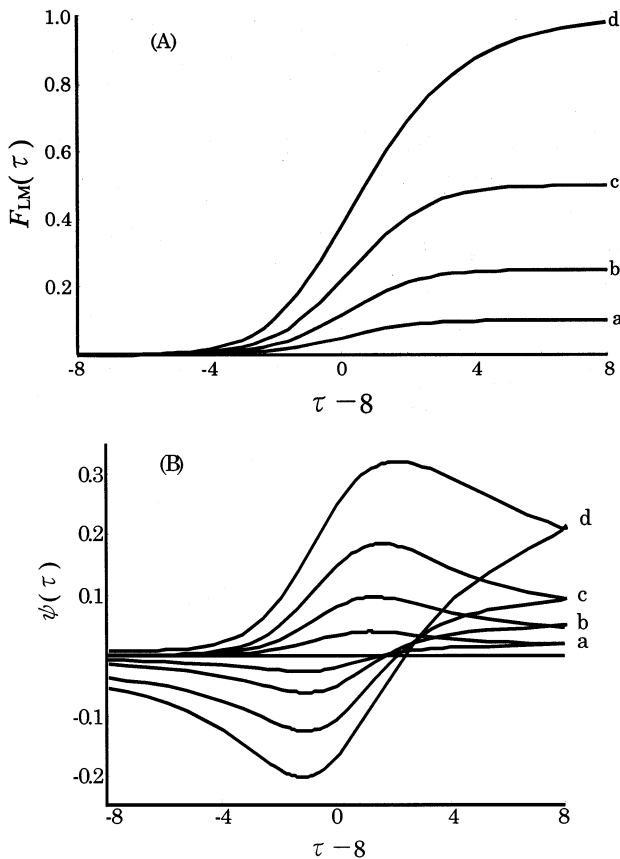


Fig. 1. Theoretical voltammograms of (A) NPV and (B) CV for $a = (a) 0.1$; (b) 0.25; (c) 0.5 and (d) 1.0. (A): $F_{LM}(\tau) = I_{(M)}^1 / zFA(D^O / \pi t_s)^{1/2} (c_L^O)^*$; $\tau = (zF/RT)\Delta E$ and $(zF/RT)(E_i - {}_r E_{1/2}) = -8$. (B): $\psi(\tau) = I^1 / (4/\pi)^{1/2} zFA(D^O v z F / RT)^{1/2} (c_L^O)^*$. $\tau = (zF/RT)vt$ and $(zF/RT)(E_i - {}_r E_{1/2}) = -8$.

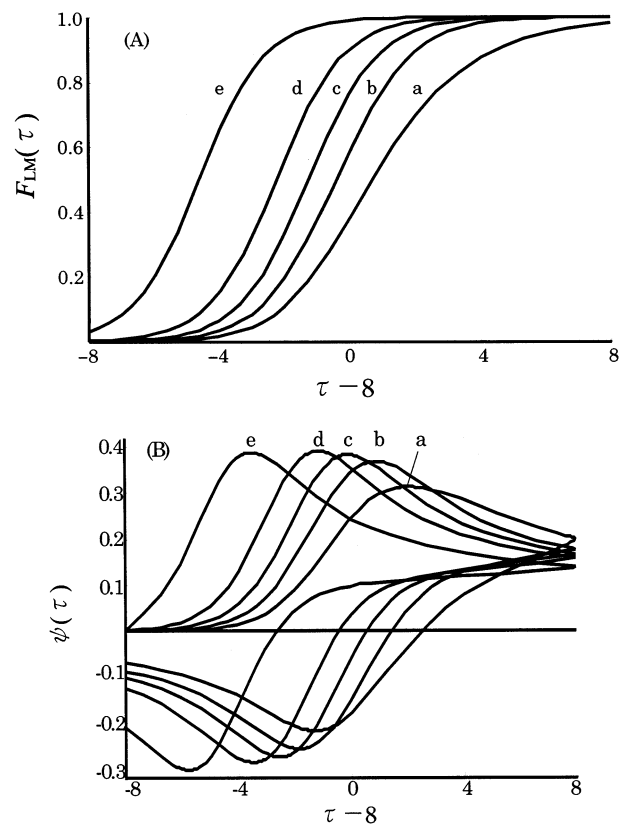


Fig. 2. Theoretical voltammograms of (A) NPV and (B) CV for $a = (a) 1$; (b) 2; (c) 4; (d) 10 and (e) 100. (A): $F_{LM}(\tau) = I_{(M)}^1 / zFA(D^O / \pi t_s)^{1/2} (c_L^O)^*$; $\tau = (zF/RT)\Delta E$ and $(zF/RT)(E_i - {}_r E_{1/2}) = -8$. (B) $\psi(\tau) = I^1 / (4/\pi)^{1/2} zFA(D^O v z F / RT)^{1/2} (c_L^O)^*$. $\tau = (zF/RT)vt$ and $(zF/RT)(E_i - {}_r E_{1/2}) = -8$.

$$I_{(M)}^1 = I_{l(M)}^1 / (1 + \exp[(fzF/RT)(E_{1/2} - E)]) \quad (13)$$

$$I_{l(M)}^1 = I_{d(M)} \quad (14)$$

$$E_{1/2}^1 = {}_r E_{1/2(M)} - (RT/zF) \ln[1 - (a/2)] \quad (15)$$

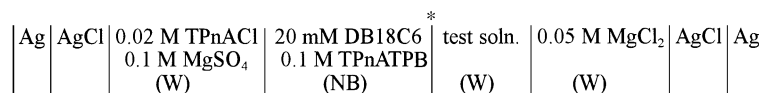
In Eq. (13), f is a constant coefficient which changes with the a -value; at $a < 0.01$, $f = 1.00$ and at $0.01 < a < 0.5$, it decreases with increasing a , as shown in Table 1, in very good approximation, but at $0.5 < a \leq 1$, f begins to depend on E more appreciably as a approaches 1. As long as f is considered to be constant, the voltammogram of CV is characterized by

$$I_{p,a(M)}^1 = 0.447zFA(D^W v f z F / RT)^{1/2} (c_M^W)^* \quad (16)$$

Table 1
The f - and f' -values in Eqs. (13), (16) and (17a,b) and Eqs. (18), (21) and (22a,b) as a function of a

| a | ≤ 0.01 | 0.1 | 0.25 | 0.5 | 1 |
|------|-------------|------|------|------|--------------------|
| f | 1.00 | 0.98 | 0.95 | 0.87 | (0.6) ^a |
| a | ≥ 100 | 10 | 4 | 2 | 1 |
| f' | 1.00 | 0.98 | 0.95 | 0.87 | (0.6) ^a |

^a Less accurate values.



Scheme 1.

$$E_{p,a(M)}^I = E_{1/2}^I + 1.11(RT/zfF) \quad (17a)$$

$$E_{p/2,a(M)}^I = E_{1/2}^I - 1.09(RT/zfF) \quad (17b)$$

Case II: when $1 \leq a$, the voltammogram of NPV is expressed by:

$$I_{(M)}^{II} = I_{1(M)}^{II} / (1 + \exp[(f'zF/RT)(E_{1/2}^{II} - E)]) \quad (18)$$

$$I_{1(M)}^{II} = I_{d(L)} = zFA(D^O/\pi t_s)^{1/2}(c_L^O)^* \quad (19)$$

$$E_{1/2}^{II} = {}_rE_{1/2(M)} - (RT/zF) \ln[a - (1/2)] \quad (20)$$

In Eq. (18), f' is a constant coefficient which changes with a ; at $a > 100$, $f' = 1$ and at $100 > a > 2$, it decreases with decreasing a , as shown in Table 1, in very good approximation, but at $2 > a \leq 1$, f' begins to depend on E more appreciably as a approaches 1. As long as f' is considered to be constant, the voltammogram of the CV is characterized by:

$$I_{pa(M)}^{II} = 0.447zFA(D^O v f' zF/RT)^{1/2}(c_L^O)^* \quad (21)$$

$$E_{p,a(M)}^{II} = E_{1/2}^{II} + 1.11(RT/f'zF) \quad (22a)$$

$$E_{p/2,a(M)}^{II} = E_{1/2}^{II} - 1.09(RT/f'zF) \quad (22b)$$

2.1. Reversibility

The voltammetric reversibility of the ionophore-assisted ion transfer as studied by NPV is examined by the wave analysis, that is, the $\ln[(I_{1(M)} - I)/I]$ vs. E plot according to Eqs. (8), (13) or (18) at $a \ll 1$ and $a \gg 1$, $0.01 < a < 0.5$ or $2 < a < 100$, respectively. At $0.5 < a < 2$, the theoretical prediction appears somewhat complicated. By CV, it is examined by the peak current height (I_p) versus $(v)^{1/2}$ plot according Eqs. (11), (16) or (21). It can be examined also by the half-peak width which is defined by $\Delta E_{p/2} = E_p - E_{p/2}$. Also, used frequently for this purpose is the peak potential separation defined by:

$$\Delta E_p = E_{p,a} - E_{p,c} \quad (23)$$

where $E_{p,a}$ is the peak potential observed at the first forward (that is, positive) scan and $E_{p,c}$ is the peak potential observed at the first backward (that is, negative) scan that follows the first forward scan after passing the switching potential, E_σ . [11] The numerical solutions indicate (a) that when $a \leq 0.01$ and $a \geq 100$, $(zF/RT)\Delta E_p = 2.3$ (error less than 0.05) when $8 > (zF/RT)(E_\sigma - E_{1/2}) > 5$, whereas (b) that at $0.01 < a < 100$, it varies with a ; $(zF/RT)\Delta E_p = 2.4, 2.5, 2.8$ and 3.4 at $a = 0.1, 0.25, 0.5$ and 1 for Case I and at $a = 10, 4, 2$ and 1 for Case II, respectively.

2.2. Half-wave potential

Experimentally, the half-wave potential is obtained by the applied potential at which $I = (1/2)I_d$ or $I = (1/2)I_1$ in NPV (see Eqs. (8), (13) and (18)). In CV, the midpoint potential defined by:

$$E_m = (E_{p,a} + E_{p,c})/2 \quad (24)$$

may be used to estimate the half-wave potential; the numerical solution indicates (a) that at $a < 0.5$ and $a > 2$, $(zF/RT)E_m$ can be equated with $(zF/RT)E_{1/2(M)}$ with an error of less than 0.05 when $8 > (zF/RT)(E_\sigma - E_{1/2}) > 5$, but the difference between the midpoint potential and the half-wave potential increases as a approaches 1; the error could be as large as $0.3(RT/zF)$ at $a = 1$.

Eq. (20) can be transformed to:

$$F^{II} = \exp[(zF/RT)({}_rE_{1/2(M)} - E_{1/2}^{II})] \quad (25)$$

$$= a - (1/2) = (D^W/D^O)^{1/2}[(c_M^W)^*/(c_L^O)^*] - (1/2)$$

$$(at a > 1) \quad (25a)$$

indicating that the F^{II} function defined by Eq. (25), when plotted against $(c_M^W)^*/(c_L^O)^*$, should give a straight line with the slope of $(D^W/D^O)^{1/2}$.

3. Experimental

3.1. NPV and CV

The electrochemical cell used can be represented by Cell I (see Scheme 1). Nitrobenzene (NB) was used as the O phase. The polarized interface, that is, the test interface is indicated by an asterisk. TPnACl and TPnATPB stand for tetrapentylammonium chloride and tetrapentylammonium tetraphenylborate, respectively. As the ionophore for K^+ - and Na^+ -ISEs, dibenzo-18-crown-6 (DB18C6) at 20 mM in NB was used, unless otherwise stated. Bis-12-crown-4(B12C4) and 2,2,3,3-tetramethyl-9-tetradecyl-14-crown-4 (TTD14C4) at 10 or 20 mM in NB were also used. Details of the reagents are described elsewhere [16,17]. A three-electrode system was used throughout the experiments. The half-wave potential of tetramethylammonium (TMA^+) ion, $E_{1/2(TMA^+)}$, was determined to be 0.36₄ V using the electrochemical cell (I) with the test solution containing 0.5 mM TMABr and 0.05 M MgCl₂. All

measurements were carried out at $25 \pm 0.1^\circ\text{C}$. Electrolysis cells and instruments are described elsewhere [16,17].

Voltammograms by NPV were recorded using a voltage pulse of 100 ms width at every $t = 3$ s and the current was sampled at the end of the voltage pulse (that is, $t_s = 100$ ms), unless otherwise stated. Voltammograms by CV were recorded using $v = 100$ mV s^{-1} , unless otherwise stated. All voltammograms were recorded after correction for the base current [16,17].

3.2. Pulse amperometry and F-pulse amperometry

For analytical purposes, a constant-height pulse voltage corresponding to the limiting current in the case of pulse amperometry [17] or to the foot of the wave in the case of F-pulse amperometry (see below) was applied to the O|W interface and the average of the sampled currents of ten successive pulses was recorded.

3.3. Stripping voltammetry

The electrochemical cell used in the stripping voltammetry of surfactants is shown by Cell II (see Scheme 2), where LiTPB denotes lithium tetraphenylborate. The polarized interface is indicated by an asterisk. In stripping voltammetry, 2-fluoro-2'-nitrodiphenylether (FNDPE) was used as the O phase, which was prepared in the form of a very thin (ca. 50 μm), poly(vinylchloride) (PVC) gel membrane on the open end of a poly(propylene) tube. The geometrical surface area of the polarized interface, that is, the electrode was 0.33 cm^2 . The gel-membrane electrode was rotated around the axis of the poly(propylene) tube usually at 300 rpm during the pre-electrolysis or pre-concentration time, t_c , when a constant pre-electrolysis potential, E_c , was applied to the FNDPE-PVC gel|test solution(W) interface, then followed by a negative potential scan to record the stripping voltammogram for determination. In the stripping voltammetry of heavy metal ions, an ionophore (see below) was added into the FNDE-PVC gel membrane. All measurements were carried out at $25 \pm 0.5^\circ\text{C}$. Further details on the reagents, preparation of gel-electrodes and electrochemical measurements are described elsewhere [19].

4. Analytical applications

4.1. NPV and CV

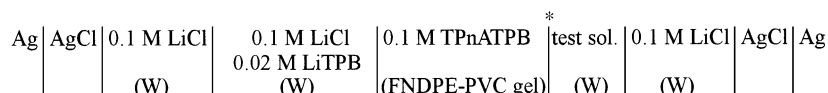
The validity of Eqs. (8)–(12) where the condition $a \ll 1$ or $a < 0.01$ is satisfied has been experimentally ascertained well and the analytical applicability of the AISEs under these conditions has also been elucidated by many authors [1–10,13]; the current response is proportional to the bulk concentration of the analyte ion in both NPV and CV, as predicted by Eqs. (9) and (11), respectively. As a exceeds 0.01, however, the current response behavior of the AISEs is not simple, as predicted by the theoretical equations of Cases I and II stated above.

The condition that $a \ll 1$ is considered to be not always satisfied since the concentration of the ionophore in the O phase may be limited by its solubility on the one hand and by economical reasons on the other. Thus, the theoretical predictions or the numerical solutions when $0.01 < a < 100$, as illustrated in Figs. 1 and 2 or predicted by Eqs. (13)–(22a,b), have been examined and actually shown to be valid with the NPV and CV behavior of DB18C6-assisted transfer of K^+ ion for $0.01 < a < 0.8$ and Na^+ ion for $1.6 < a < 16$ at the 20 mM DB18C6(NB)|0.05 M $\text{MgCl}_2(\text{W})$ interface (data not shown, see figs. 3 and 4 in [18]). Similar experimental results by CV with DB18C6-assisted transfer of K^+ ion at the 1,2-dichloroethane|W interface have been reported by Beattie et al. [15]. The half-wave potential of Na^+ ion estimated by Eq. (24) has also been proved to satisfy Eq. (25) for $1.6 < a < 16$, giving $(D^{\text{W}}/D^{\text{NB}})^{1/2} = 1.58 \pm 0.03$ for Na^+ ion at the 20 mM DB18C6|0.05 M $\text{MgCl}_2(\text{W})$ interface [18].

When $a > 100$, the predictions of Eqs. (18)–(22a,b) with $f' = 1$ have been shown to be valid with the NPV and CV behavior of DB18C6-assisted transfer of Na^+ ion at the 0.1–2 mM DB18C6(NB)|50–100 mM $\text{NaCl}(\text{W})$ interface (data not shown, [18]).

4.2. Pulse amperometry and F-pulse amperometry

In analytical applications, the pulse amperometric technique, in which a constant height pulse potential corresponding to the limiting current of NPV is applied to the O|W interface, can be used advantageously [4,5,17]. When $a < 0.01$, the response current is proportional to $(c_M^{\text{W}})^*$ as is expected from Eq. (9). With



Scheme 2.

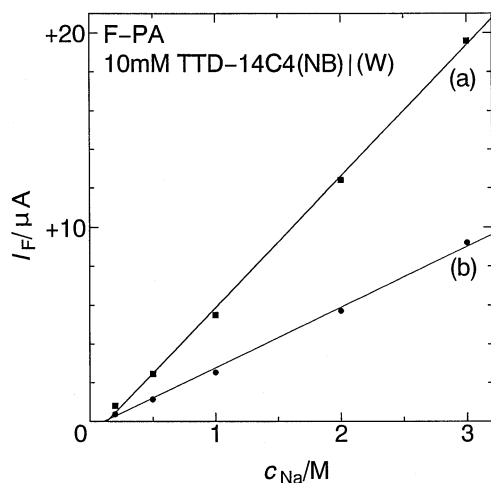


Fig. 3. Plots of the F-pulse currents (I_F) at E_F = (a) 0.28 and (b) 0.26 V with $E_i = 0.20$ V against the concentration (c_{Na}) of NaCl in 0.1 M MgCl_2 , 0.05 M CaCl_2 , 0.08 M KCl (W) at the 10 mM TTD14C4(NB) | (W) interface.

increased a , however, particularly when $a > 1$, the current response is not proportional to $(c_M^W)^*$ but rather to $(c_M^W)^*$ as predicted by Eq. (19). Even when $a < 1$, the current versus potential curve will be drowned out, resulting in decreased precision in the determination of the current height. Thus, for Cases I and II, the F-pulse amperometry has been proposed [18], in which a constant-height pulse potential corresponding to the foot of the wave is applied to the interface. The current is sampled by the same procedure as in NPV. If the pulse potential E_F is the potential at which the theoretical current $I_{F(M)}$ ($= I_{(M)}^I$ or $I_{(M)}^{II}$ at $E = E_F$ in Eqs. (13) or (18), respectively) is negligibly small compared with the theoretical limiting current $I_{d(L)}$ defined by Eq. (19), that is, when $I_{F(M)} \ll I_{d(L)}$, it can be shown that the sampled currents in Case I and II are given, respectively, by:

Case I:

$$I_{F(M)}^I = I_{d(M)} / (1 + \exp[(zF/RT)({}_rE_{1/2(M)} - E_F)]) \quad (26)$$

Case II:

$$I_{F(M)}^{II} = I_{d(M)} \exp[(zF/RT)(E_F - {}_rE_{1/2(M)})], \quad (27)$$

where $I_{d(M)}$ is defined by Eq. (9). Therefore, we can expect that the F-pulse amperometric current is proportional to the bulk concentration of the analyte ion, though the cost of this is that the current response is theoretically dependent on the applied potential. It is noted that Eq. (26) is reduced to Eq. (27) with an error of less than 1% when $(zF/RT)({}_rE_{1/2(M)} - E_F) > 4.6$. The predicted linearity of calibration curves according to Eqs. (26) and (27) has been tested successfully with test solutions, such as 1.0 ~ 20 mM KCl in 50 mM

MgCl_2 (W) and 20–200 mM NaCl in 50 mM MgCl_2 (W) at the 20 mM DB18C6(NB) | (W) interface and others (data not shown, see [18]), all giving linear calibration curves in the concentration ranges stated. The linearity has been proved even with test solutions of more concentrated analyte ion; 0.2–3 M NaCl in 0.08 M KCl, 0.05 M CaCl_2 + 0.1 M MgCl_2 (W) at the 10 mM TTD14C4(NB) | (W) interface, as shown in Fig. 3. The regression lines for the calibration curves obtained at $E_F = 0.26$ and 0.28 V can be expressed, respectively, by:

$$I_F(0.26 \text{ V})/\mu\text{A} \\ = (-0.34 \pm 0.13) + (3.12 \pm 0.08)(c_{\text{Na}}^W)^*/\text{M}$$

and

$$I_F(0.28 \text{ V})/\mu\text{A} \\ = (-0.90 \pm 0.25) + (6.75 \pm 0.14)(c_{\text{Na}}^W)^*/\text{M}$$

The ratio of the slope (at 0.28 V) to the slope (at 0.26 V) of the calibration curves is 2.16 ± 0.07 , whereas the calculated value of the ratio by Eq. (27) is 2.18.

Application of PISEs to the quantification of ions at extremely high concentration like the on-line monitoring of brine composition in salt-making factories has been studied, in which the correction of the potential response for (activity coefficients due to) high ionic strength is required [20]. The current response (I) of AISEs depends on the diffusion coefficient of ionic species, as expressed by Eqs. (9) and (14), which can be summarized as

$$I = k'_{\text{amp}}(D^W)^{1/2}(c_M^W)^* \quad (k'_{\text{amp}} = \text{a constant}) \quad (28)$$

All theoretical equations considered in this paper are derived by assuming the presence of sufficient amounts of supporting electrolyte in the W phase (so that a constant diffusion coefficient or constant activity coefficient and negligible migration can be assumed), which is not always in harmony with the experimental conditions, particularly with those in concentrated solutions of analyte ion where F-pulse amperometry may be used. The dependence of the diffusion coefficient in concentrated aqueous solutions on their increased ionic strength appears not very appreciable [21]. In F-pulse amperometry, however, k'_{amp} in Eq. (28) is a function of $(zF/RT)({}_rE_{1/2(M)} - E_F)$ while ${}_rE_{1/2(M)}$ is expected to change with $(D^W)^{1/2}$ (see Eq. (10)) and γ_M^W is the activity coefficient of analyte ion M in the W phase [13]. Both D^W and γ_M^W may change with $(c_M^W)^*$, particularly in concentrated solutions of analyte ion. Interestingly, by introducing the theoretical dependence of ${}_rE_{1/2(M)}$ on $(D_M^W)^{1/2}$ and γ_M^W into Eq. (27), Eq. (28) is transformed into another expression: $I = k''_{\text{amp}}\gamma_M^W(c_M^W)^*$, k''_{amp} being a constant. The experimental linear calibration curves such as illustrated in Fig. 3 and others [18] could be attributed to fortuitous compensation.

4.3. Stripping voltammetry

The ion-transfer stripping voltammetry technique seems promising for the electrochemical determination of heavy metal ions at trace level. Thus, it has been shown [19] that Hg^{2+} ion at a concentration level as low as 8 nM or 1.6 ppb can be determined using the 0.01 M HTCO (FNDPE-PVC gel) | (W) electrode interface (HTCO: 1,4,7,10,13,16-hexathiacyclooctadecane). The method can be extended to the determination of Pb^{2+} ion at ppb level [19,22]. Determination of Zn^{2+} , Cd^{2+} and Pb^{2+} ions at trace level can be done also by stripping voltammetry based on DPT-assisted transfer of the ions at the O-gel | W interface (DPT: 5,6-diphenyl-3-(2-pyridyl)-triazine) [22].

In this paper, ion-transfer stripping voltammetry applied to the determination of a poly(oxyethylene)alkyl ether (CmEn: $\text{C}_m\text{H}_{2m+1}-\text{O}(\text{CH}_2\text{CH}_2\text{O})_n\text{H}$) surfactant at trace level is described. It can be shown that the nonionic surfactant can be transferred electrochemically across the O-gel | W interface in the presence of such ions as Na^+ , K^+ , Mg^{2+} , Ca^{2+} , Ba^{+2} or La^{3+} in the W phase within the potential window. This is probably due to the coordination of the polyether chain to the cations to form a complex similar to that of a cation with a crown ether-type ionophore [23–26]. Thus, the trace determination of the surfactant can be carried out based on the ion-assisted, anodic pre-concentration of the surfactant into the thin O-gel layer followed by cathodic stripping voltammetry, as shown, for example, by Fig. 4 curve a, which was obtained with a test solution of 200 nM C12E7 in 20 mM NaCl under the experimental conditions described. The cathodic stripping peak current is proportional to the

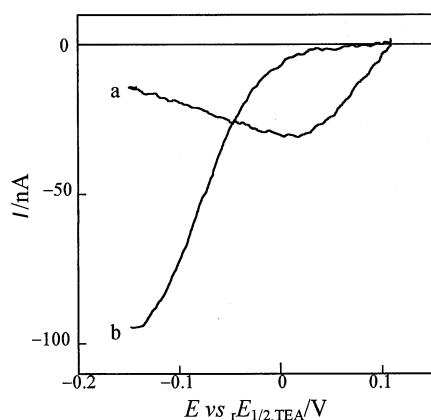


Fig. 4. (a) A cathodic stripping voltammogram of 0.2 μM C12E7 in 20 mM NaCl(W) at the FNDPE-PVC gel electrode following pre-concentration at $E_c = 0.11$ V for $t_c = 300$ s under stirring of $N = 300$ rpm. (b) A negative potential sweep voltammogram of 2 μM SDS in 20 mM NaCl(W) at the same electrode at $N = 300$ rpm. All voltammograms, corrected for the base currents, were recorded at $\nu = 0.01$ V s^{-1} .

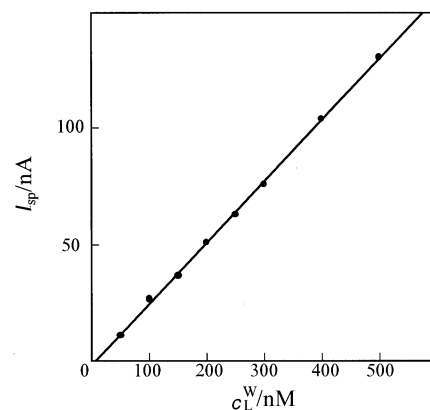


Fig. 5. Plot of the cathodic stripping peak current (I_{sp}) against the concentration (c_L^W) of C12E7 in 10 mM KCl(W) at the FNDPE-PVC gel electrode. $E_c = 0.08$ V, $t_c = 120$ s, $N = 300$ rpm, and $\nu = 0.01$ V s^{-1} .

concentration of the surfactant in the test solution. Fig. 5 shows a calibration curve of 50–300 nM C12E7 obtained under the experimental conditions described in the caption. Also, Fig. 4 curve b shows a cathodic voltammogram produced by 2 μM SDS (SDS: sodium dodecyl sulfate) in 20 mM NaCl, indicating that the separate determination of the nonionic and anionic surfactants is allowed by use of the voltammetric technique.

5. Conclusions

AISEs can be applied to the quantification of analyte ion (or ions) at concentration levels from molar to nanomolar. The current response is linear with the concentration of the analyte and additive with respect to the contributions of each of the active components present in the test solution. The additivity allows, in principle when their half-wave potentials are reasonably separated, the separate determination of the two or more components or the elimination of the interference with them. The electrochemical study of ion transfer reactions at the O | W interface provides the basic principles of electrochemical or electro-assisted solvent extraction, or, in short, electroextraction or electro-partition of ionic species, which can be used for the separation or pre-concentration of ion or ions in analytical applications [27].

Acknowledgements

This work was supported by a Grant-in-Aid from Fukui-ken University Science Foundations (Nos. 25 and 35), for which the authors (M.S. and H.K.) are very grateful.

References

- [1] M. Senda, T. Kakiuchi, T. Osakai, *Electrochim. Acta* 36 (1991) 253.
- [2] H.H. Girault, in: J.O'M Bockris, B. Conway, R. White (Eds.), *Modern Aspects of Electrochemistry* No. 25, Plenum Press, New York, 1993, p. 1.
- [3] M. Senda, *Denki Kagaku* 63 (1995) 368.
- [4] M. Senda, Y. Yamamoto, in: A.G. Volkov, D.W. Deamer (Eds.), *Liquid|Liquid Interfaces. Theory and Methods*, CRC Press, Boca Raton, 1996, p. 276.
- [5] M. Senda, in: F.W. Scheller, F. Schubert, J. Fedrowitz (Eds.), *Frontiers in Biosensorics. I. Fundamental Aspects*, Birkhäuser Verlag, Basel, 1997, p. 193.
- [6] M.D. Osborne, Y. Shao, P.M. Pereira, H.H. Girault, *J. Electroanal. Chem.* 364 (1994) 155.
- [7] B. Hundhammer, T. Solomon, T. Zerihun, M. Abegaz, A. Bekele, K. Graichen, *J. Electroanal. Chem.* 371 (1994) 1.
- [8] S. Sawada, T. Osakai, M. Senda, *Anal. Sci.* 11 (1995) 733.
- [9] S. Wilke, H.M. Wang, M. Muraczewska, H. Mueller, *Fresenius J. Anal. Chem.* 356 (1996) 233.
- [10] H.J. Lee, C. Beriet, H.H. Girault, *Anal. Sci.* 14 (1998) 71.
- [11] R.S. Nicholson, I. Shain, *Anal. Chem.* 36 (1964) 706.
- [12] H. Matsuda, Y. Yamada, K. Kanamori, Y. Kudo, Y. Takeda, *Bull. Chem. Soc. Jpn.* 64 (1991) 1497.
- [13] T. Kakutani, T. Osakai, M. Senda, *Bull. Chem. Soc. Jpn.* 56 (1983) 391.
- [14] H. Matsuda, Y. Ayabe, *Z. Elektrochem.* 59 (1955) 494.
- [15] P.D. Beattie, R.G. Wellington, H.H. Girault, *J. Electroanal. Chem.* 396 (1995) 317.
- [16] H. Katano, M. Senda, *Bull. Chem. Soc. Jpn.* 70 (1997) 2489.
- [17] T. Osakai, T. Nuno, Y. Yamamoto, A. Saito, M. Senda, *Bunseki Kagaku* 38 (1989) 479.
- [18] M. Yamada, H. Katano, M. Senda, *Bunseki Kagaku* 47 (1998) 919.
- [19] H. Katano, M. Senda, *Anal. Sci.* 14 (1998) 63.
- [20] N. Yoshikawa, *Bunseki Kagaku* 46 (1997) 633.
- [21] R.A. Robinson, R.H. Stokes, *Electrolyte Solutions*, 2nd edition, Butterworths, London, 1959, p. 515.
- [22] H. Katano, M. Senda, in preparation for publication.
- [23] K. Toei, S. Motomizu, T. Umano, *Talanta* 29 (1982) 103.
- [24] N. Kojima, paper presented at the 4th Analytical Chemistry Forum in Hokuriku, Takaoka, Nov. 7–8, 1997.
- [25] Z. Yoshida, S. Kihara, *J. Electroanal. Chem.* 227 (1987) 171.
- [26] T. Kakiuchi, *J. Electroanal. Chem.* 345 (1993) 191.
- [27] M. Senda, T. Kakutani, *Hyomen (Surface)* 18 (1980) 535.